© MAY 2026 | IRE Journals | Volume 9 Issue 11 | ISSN: 2456-8880
DOI: https://doi.org/10.64388/IREV9I11-1717868

Rudiment of operation of Controlled Three-phase full-wave Rectifier

EZEMA E.E.[1], [2]EJIMOFOR I. A[2], ABBA M.O.[3]
[1]*Department of Electrical/Electronic Engineering, Faculty of Engineering Madonna University, Nigeria.*
[2]*Department of Computer Engineering, Faculty of Engineering, Madonna University, Nigeria*
[3]*Dept of Electrical Engineering, Enugu State University of Science & Technology (ESUT), Enugu, Nigeria*

Abstract- ***Three-phase bridge rectifier circuits are extensively used in many high-power, low-cost applications over a wide range of both electronic and electrical power industries up to the 120kW level. They are applied in brushless excitation system for aircraft generators, static generator excitation schemes, road vehicle generator systems, high voltage ac-dc power conversion, and in wide range of d. c. motor and a. c. motor drives. Three-phase full-wave rectifier performance is examined in this paper. The output voltage is controlled by the firing angle δ. There is a constant connection between the currents and voltages on the a. c. side and the currents and voltages on the d. c. side. The circuit equations are derived for the input quantities, and output quantities, based on a series RL load.***

Keywords: controlled three-phase rectifier, delay angle, six-pulse, continuous conduction, inductive load

I. INTRODUCTION

Fig. 1 shows a controlled six-pulse three-phase converter [1]-[4]. Controlled rectifiers are employed in many industrial schemes such as dc motor drives, electromechanical and electrometallurgical processes, magnet power supplies, dc transmission, portable hand tools, and uninterruptible power supplies [5]-[6].

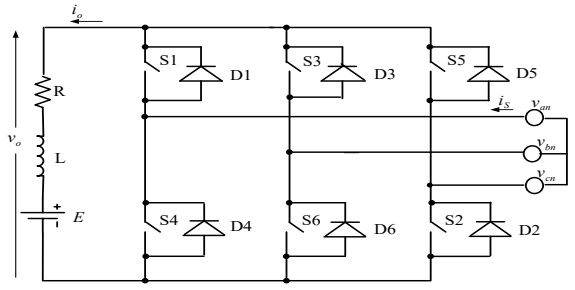

Fig. 1 Six-pulse fully controlled three-phase rectifier

There are six pulses of the output voltage per cycle, hence the description "six-pulses" [7]. The Current continuity has the positive effects of reducing the current ripples, and hence torque ripples in a motor [8]. Conduction begins when a gate signal is applied while the switch is forward biased. Switches are fired in the sequence they are numbered, with a phase difference of 60o. Only two switches conduct at a time – one odd-numbered and one even-numbered [9]-[10]. Any of these line-to-line voltages appears as an output voltage vo across the load when the appropriate switches conduct. For example, if S1 and S6 conduct simultaneously, then line voltage vab is applied across the load. The three-phase controlled rectifier provides two-quadrant operation, where the polarity of the output voltage can be positive or negative. The waveforms of the line-to-line voltages are shown in Fig. 2. At vab acquires a greater positive value than any of the other five source voltages.

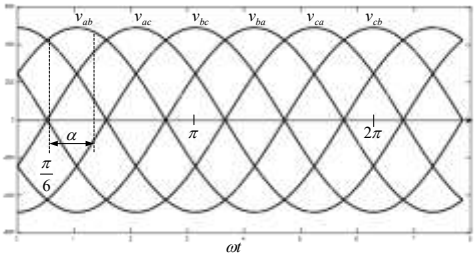

Fig. 2 Waveforms of source line-to-line voltages.

II. SUPPLIED-SIDE QUANTITY

The instantaneous input current of a phase can be expressed in Fourier series.

© MAY 2026 | IRE Journals | Volume 9 Issue 11 | ISSN: 2456-8880
DOI: https://doi.org/10.64388/IREV9I11-1717868

$$i_s(t) = I_{dc} + \sum_{n=1\ldots}^{\infty}(a_n \cos n\omega t + b_n \sin n\omega t)$$

(1)

$$I_{dc} = \frac{a_0}{2} = \frac{1}{2\pi}\int_0^{2\pi} i_s(t)d\omega t = \frac{1}{2\pi}\int_{\frac{\pi}{6}+\alpha}^{\frac{5\pi}{6}+\alpha} I_a d\omega t - \int_{\frac{7\pi}{6}+\alpha}^{\frac{11\pi}{6}+\alpha} I_a d\omega t = 0$$

(2)

$$a_n = \frac{1}{\pi}\int_0^{2\pi} i_s(t)\cos n\omega t\, d(\omega t) = \frac{1}{\pi}\left[\int_{\frac{\pi}{6}+\alpha}^{\frac{5\pi}{6}+\alpha} I_a \cos n\omega t\, d(\omega t) - \int_{\frac{7\pi}{6}+\alpha}^{\frac{11\pi}{6}+\alpha} I_a \cos n\omega t\, d(\omega t)\right]$$

(3)

$$i_s(t) = \sum_{n=1\ldots}^{\infty} C_n \sin(n\omega t - n\alpha) = \sum_{n=1\ldots}^{\infty} C_n \sin(n\omega t + \theta_n)$$

(4)

Where

$$C_n = \sqrt{a_n^2 + b_n^2} \quad (5)$$

$$\theta_n = \tan^{-1}\frac{a_n}{b_n} = -n\alpha \quad (6)$$

The rms value of the n^{th} harmonic input current is:

$$I_{sn} = \frac{C_n}{\sqrt{2}} \quad (7)$$

The rms value of the fundamental current is:

$$I_{s1} = \frac{\sqrt{6}\, I_a}{\pi} \quad (8)$$

The rms value of the input current is given as:

$$I_s = \left[\sum_{n=1}^{\infty} I_{sn}^2\right]^{\frac{1}{2}} \quad (9)$$

The total harmonic distortion (THD) of the input current is given by:

$$THD = \left[\left(\frac{I_s}{I_{s1}}\right)^2 - 1\right]^{\frac{1}{2}} \quad (10)$$

The waveform of the supply-side current i_s for $\alpha = 30^o$ is shown in Fig. 3

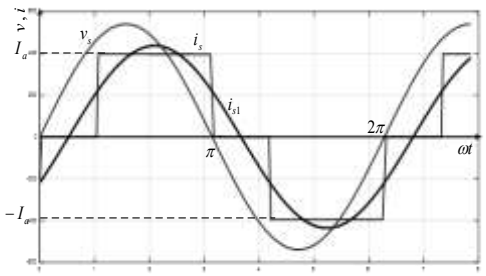

Fig. 3 Waveform of supply line current (is), for. $\alpha = 30^o$ i_{s1} is fundamental component, and $I_a = I_o$. The THD of the input current is found to be 31%; and the power factor is equal to 0.89

The rectifier draws pulsed; fluctuating current is from the utility grid. These non-sinusoidal currents produce significant harmonic pollution, poor power factor, and voltage drop across the finite internal grid impedance and the voltage waveform in the vicinity becomes distorted [11]-[15]. Many strategies and topologies have been proposed to deal with this problem so as to meet the requirement of the standards. Among them are multi-pulse schemes due to their reliability, compactness, and effectiveness. Large ac input filter is also used to reduce high-frequency input current ripples.

III. OUTPUT QUANTITIES

The output voltage is given as:

$$v_o = V_o + \sum_{n=1}^{\infty}(a_n \cos n\omega t + b_n \sin n\omega t)$$

(11)

Where

Average output voltage of the rectifier is:

$$V_o = \frac{1}{\pi/3}\int_{\frac{\pi}{6}+\alpha}^{\frac{\pi}{2}+\alpha} \sqrt{3}\, V_m \sin\left(\omega t + \frac{\pi}{6}\right) d\omega t$$

(12)

The average load current is given by:

$$I_o = \frac{V_o - E}{R} \quad (13)$$

$$a_n = \frac{1}{\pi}\left\{\begin{array}{l}\int_{\frac{\pi}{6}+\alpha}^{\frac{\pi}{2}+\alpha} v_{ab}\cos n\omega t\, d\omega t + \int_{\frac{\pi}{2}+\alpha}^{\frac{5\pi}{6}+\alpha} v_{ac}\cos n\omega t\, d\omega t + \int_{\frac{5\pi}{6}+\alpha}^{\frac{7\pi}{6}+\alpha} v_{bc}\cos n\omega t\, d\omega t + \\ \int_{\frac{7\pi}{6}+\alpha}^{\frac{9\pi}{6}+\alpha} v_{ba}\cos n\omega t\, d\omega t + \int_{\frac{9\pi}{6}+\alpha}^{\frac{11\pi}{6}+\alpha} v_{ca}\cos n\omega t\, d\omega t + \int_{\frac{11\pi}{6}+\alpha}^{\frac{13\pi}{6}+\alpha} v_{cb}\cos n\omega t\, d\omega t\end{array}\right\}$$

(14)

$$b_n = \frac{1}{\pi}\left\{\begin{array}{l}\int_{\frac{\pi}{6}+\alpha}^{\frac{\pi}{2}+\alpha} v_{ab}\sin n\omega t\, d\omega t + \int_{\frac{\pi}{2}+\alpha}^{\frac{5\pi}{6}+\alpha} v_{ac}\sin n\omega t\, d\omega t + \int_{\frac{5\pi}{6}+\alpha}^{\frac{7\pi}{6}+\alpha} v_{bc}\sin n\omega t\, d\omega t + \\ \int_{\frac{7\pi}{6}+\alpha}^{\frac{9\pi}{6}+\alpha} v_{ba}\sin n\omega t\, d\omega t + \int_{\frac{9\pi}{6}+\alpha}^{\frac{11\pi}{6}+\alpha} v_{ca}\sin n\omega t\, d\omega t + \int_{\frac{11\pi}{6}+\alpha}^{\frac{13\pi}{6}+\alpha} v_{cb}\sin n\omega t\, d\omega t\end{array}\right\}$$

(!5)

$$i_o = \sum_{n=1}^{\infty}\frac{1}{Z_n}\left[a_n\cos\left(n\omega t-\theta_n\right)+b_n\sin\left(n\omega t-\theta_n\right)\right]$$

(16)

$$Z_n = \sqrt{R^2+\left(n\omega L\right)^2} \qquad (17)$$

$$\theta_n = \tan^{-1}\left(\frac{n\omega L}{R}\right) \qquad (18)$$

The output voltage vo and current io are shown in Fig. 4.

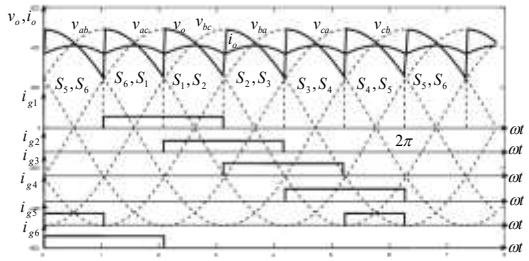

Fig.4 Output voltage (v_o) and current (i_o), gate signals, and source voltages

These plots are typical conditions of continuous-current operation. Fig. 5 shows the waveforms when α = 90°. Thus as α increases, the converter operation tends to inversion.

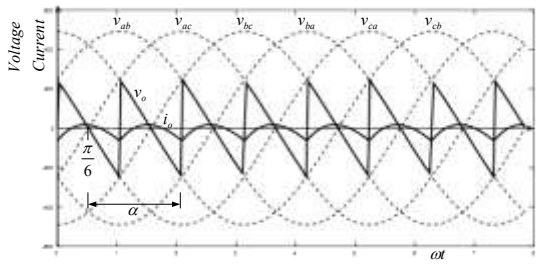

Fig. 5 Output voltage and current for α = 90o

IV. CONCLUSION

The performance of controlled three-phase rectifier feeding an inductive load has been carried out in this paper. The average output voltage could be either positive or negative according to the value of α. When α exceeds 90o, the output voltage becomes negative, and the rectifier enters inversion mode. The total harmonic distortion (THD) of the input current is high (THD = 31%); and so, multi-pulse configurations or large ac input filters can be used to mitigate the effects of harmonic pollution.

REFERENCES

[1] Yuan-Chih Chang, Chien-Hua Chen, Zhong Chuan Zhu, and Yi-Wien Huang, "Speed Control of the Surface-Mounted Permanent-Magnet Synchronous Motor Based on Takagi-Sugeno Fuzy Models," IEEE Transaction on Power Electronics, vol. 31, No. 9, September, 2016, pp. 6504-6510.

[2] G. Tan, X. Wu, Z. Wang, and Z. Ye, "A Generalized Algorithm to Eliminate Spikes of Common-Mode Voltages for CMVRPWM," IEEE Transaction on Power Electronics, vol. 31, No. 9, September, 2016, pp. 6698-6709.

[3] T. Mannen, and H. Fujita, "Dynamic Control and Analysis of DC-Capacitor Voltage Fluctuations in Three-Phase Active Power Filters," IEEE Transaction on Power Electronics, vol. 31, No. 9, September, 2016, pp. 6710-6718.

[4] J. Shang, and Y. Wei Li, "A Space-Vector Modulation Method for Common-Mode Voltage Reduction in Current-Source Converters," IEEE Transaction on Power

Electronics, vol. 29, No.1, January, 2014, pp. 374-385.

[5] S. B. Dewan, A. Straughen, Power Semiconductor Circuits, New York: John Wiley & Sons, Inc., 1975, pp. 214-229.

[6] M. Pichan, A. A. Ahamad, A. Arishamifar, and M. E. Jamarani, "A straightforward Procedure to Select Passive Elements in Single-phase Pulse-width Modulation Rectifiers with Developed Resonant Current Controller," Electric Power Components and Systems, 44(4):379-389, 2016.

[7] A. Hughes and B. Drury, Electric Motor Drives – Fundamentals, Types, and Applications, Fourth Edition, Elsvier, Oxford, 2013, pp. 57

[8] R. Krishnan, Electric Motor Drives – Modeling, Analysis, and Control, Prentice Hall, New Jersey, 2001, pp. 51-52.

[9] Dubey G.K., Power Semi-conductor Controlled Drives, Prentice Hall, N.J. 1989.

[10] M. H. Rashid, Power Electronics-Circuits, Devices, and Applications, second edition, New Jersey: Prentice-Hall, Inc., 1988, pp. 138-142.

[11] C. Qiao, and K. M. Smeldley, "A General Three-phase PFC Controller for Rectifiers with Parallel-Connected Dual Boost Topology," IEEE Transactions on Power Electronics, vol. 17, no. 6, November 2002, pp. 925-934.

[12] J. Allmeling, "A control Structure for Fast Harmonics Compensation in Active Filters," IEEE Transaction on Power Electronics, vol. 19, March 2004, pp. 508-514.

[13] J. A. G. Marafao, J. A. Pomilio, and G. Spiazzi, "Improved Three-Phase High-Quality Rectifier with Line-Commutated Switches," IEEE Transaction on Power Electronics, vol. 19, May, 2004, pp. 640-648.

[14] V. A. Katic, and D. Graovac, "A Method for PWM Rectifier Line Side Filter Optimization in Transient and Steady State," IEEE Transaction on Power Electronics, vol. 17, no. 3, 2002, pp. 342-352

[15] Chung-Ming Young, Sheng-Feng Wu, Wei-Shan Yeh, and Cheng-Wei Yeh, "A DC-Side Current Injection Method for Improving AC Line Condition Applied in the 18-Pulse Converter System," IEEE Transaction on Power Electronics, vol. 29, no. 1, January 2014, pp. 99-109.